Electronic Supplementary Information

Vertical graphene growth on uniformly dispersed sub-nanoscale SiOx/N-doped carbon composite microspheres with a 3D conductive network and an ultra-low volume deformation for fast and stable lithium-ion storage

Meisheng Han[1a,b], Yongbiao Mu[1a], Fu Yuan,[a] Jingbing Liang,[a] Tao Jiang,[a] Xuedong Bai[b], and Jie Yu*[a,c]

[a]Songshan Lake Materials Laboratory Dongguan, Guangdong 523808,China
[b]Beijing National Laboratory for Condensed Matter Physics, Institute of Physics, Chinese Academy of Sciences, Beijing 100190, China
[c]Shenzhen Engineering Lab for Supercapacitor Materials, Shenzhen Key Laboratory for Advanced Materials, School of Material Science and Engineering, Harbin Institute of Technology, Shenzhen, University Town, Shenzhen 518055, China
*Corresponding Author.
E-mail address: jyu@hit.edu.cn (J. Yu);
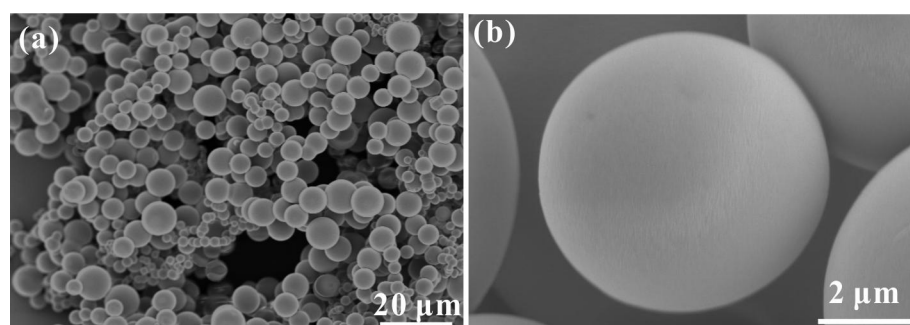[1]Both authors contributed equally to this work.

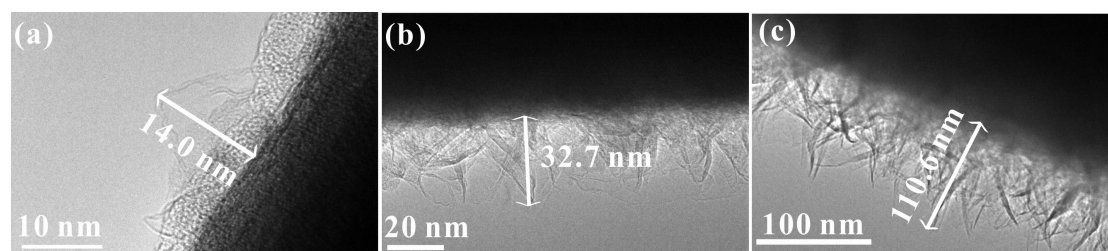**Fig. S1** SEM images of SiOCN spheres.

Fig. S2 Transmission electron microscope (TEM) images of VG@SiOx/NC obtained at 1100 °C with a 6.25% volume ratio of CH_4 in the mixture gas of CH_4 and H_2 with different growth time (a) 4 h, (b) 6 h, and (c) 8 h.
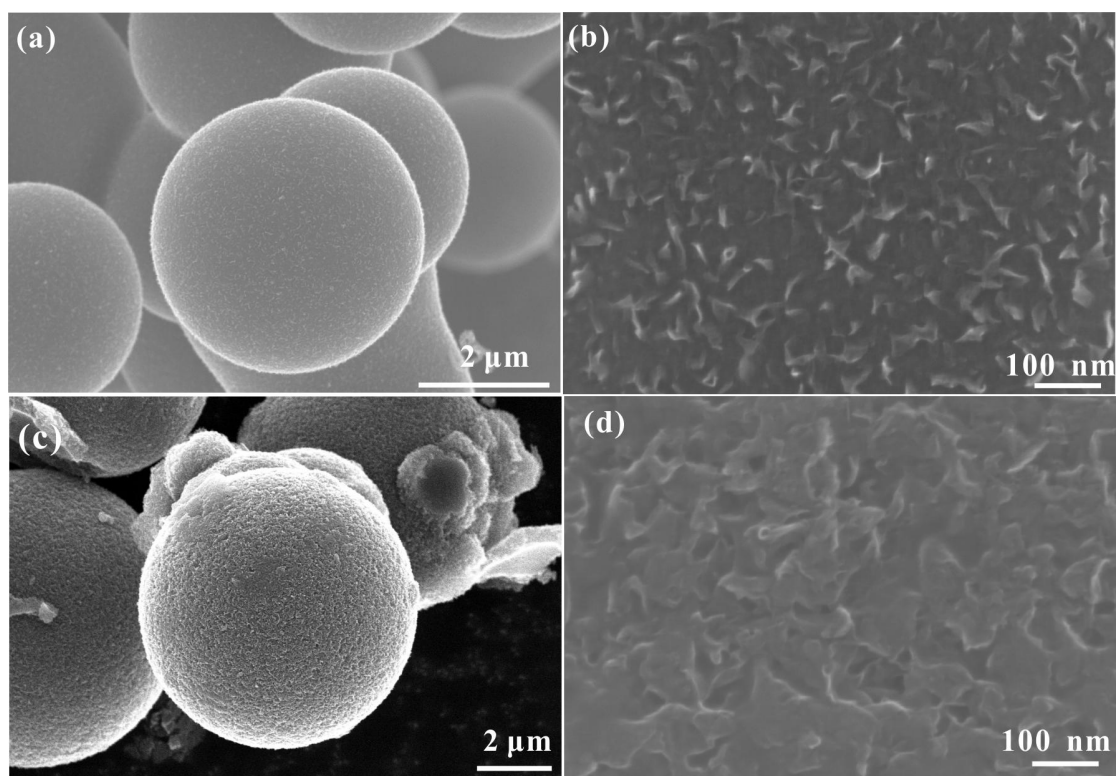
Fig. S3 SEM images of VG@SiO$_x$/NC obtained at 1100 ºC for 8 h in different volume ratios of CH$_4$ in the mixture gas of CH$_4$ and H$_2$ (a,b) 5% and (c,d) 8.5%.
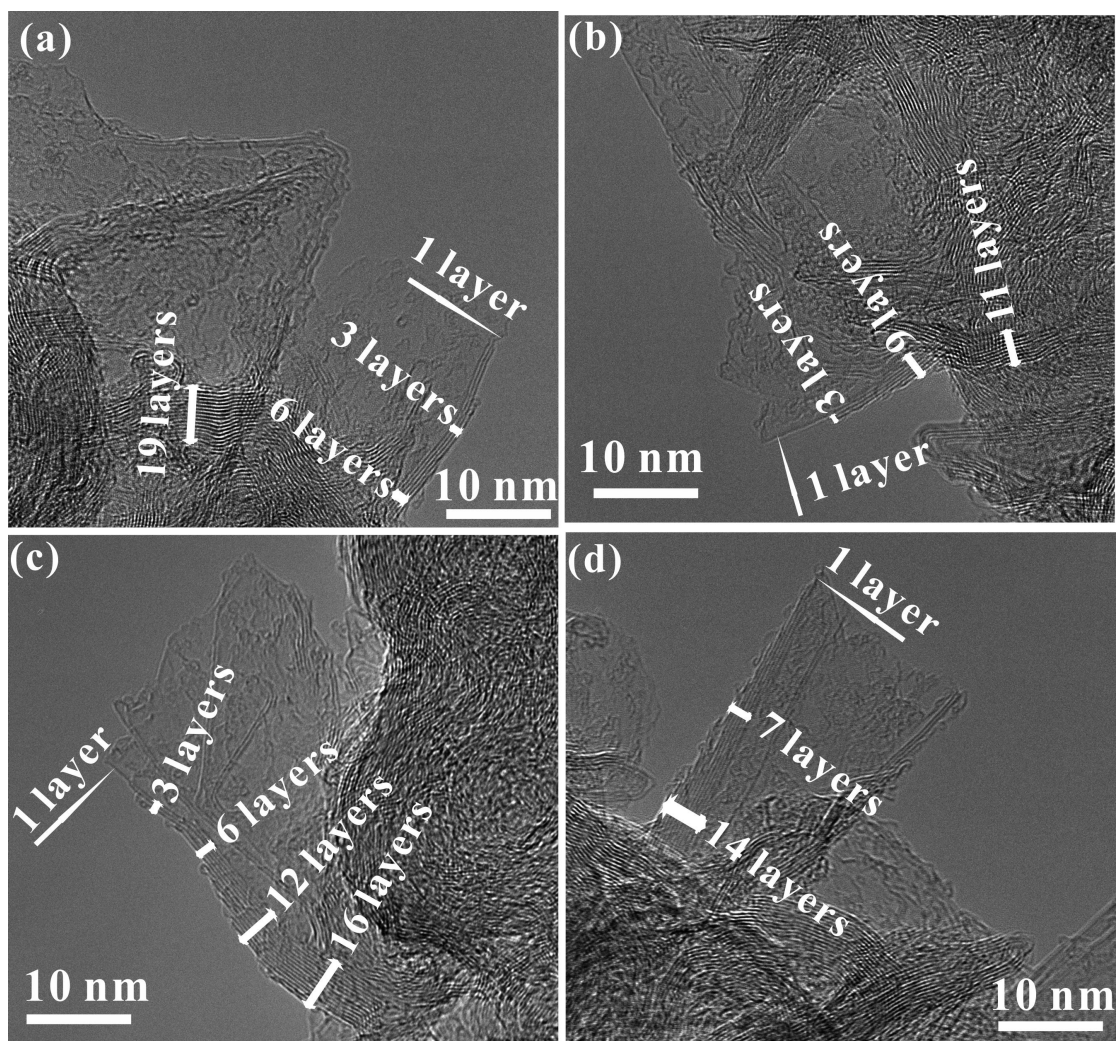
Fig. S4 High resolution transmission electron microscope images of edge of VG@SiO$_x$/NC obtained at 1100 ^{o}C for 8 h in 6.25% volume ratio of CH$_4$ in the mixture gases of CH$_4$ and H$_2$.
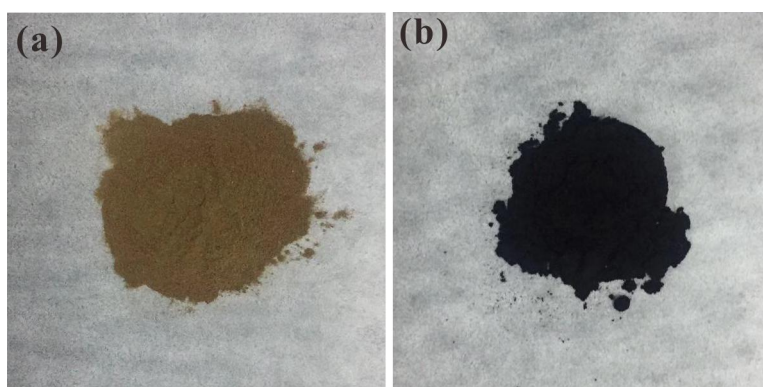

Fig. S5 The optical images of SiOCN (a) and SiO$_x$/NC (b).

Table S1 Chemical composition of the obtained samples from elemental analysis results.

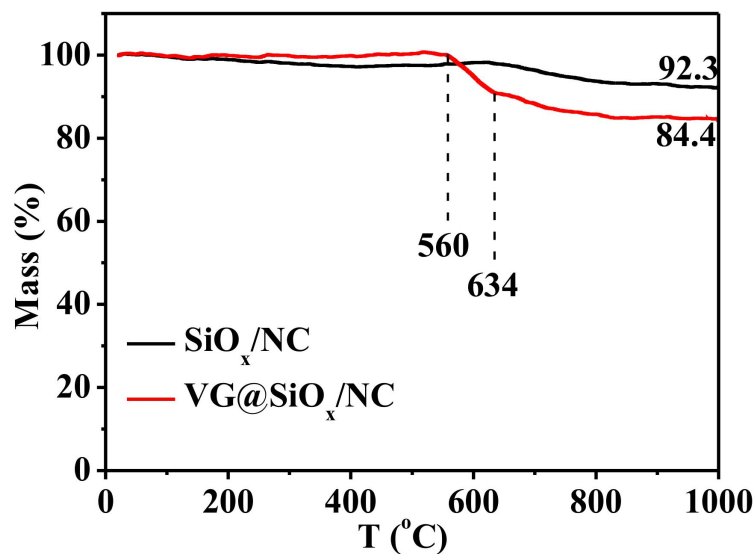| Samples	Si (wt/at%)	O (wt/at%)	C (wt/at%)	N (wt/at%)	H (wt/at%)
SiOCN	41.0/16.5	16.7/11.7	32.7/30.7	6.4/5.1	3.2/36.0
SiO_x/NC	43.3/26.5	17.9/19.2	33.2/47.4	5.6/6.9	0/0
VG@SiO_x/NC	39.9/23.6	16.4/17.0	38.4/53.1	5.3/6.3	0/0

Fig. S6 TG curves of SiO_x/NC and VG@SiO_x/NC. The testing conditions are that samples were heated from room temperature to 1000 °C at a heating rate of 2 °C min^{-1} in air atmosphere.
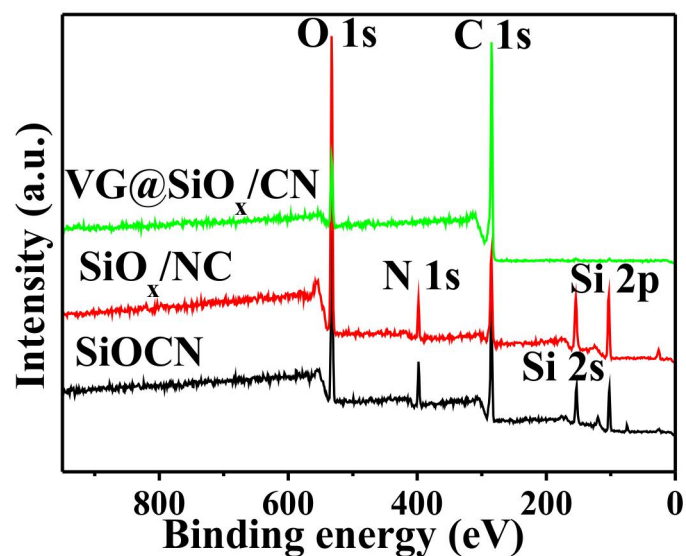

Fig. S7 XPS survey peaks of samples.

Table S2 Fitting results of XPS spectra of the obtained samples.

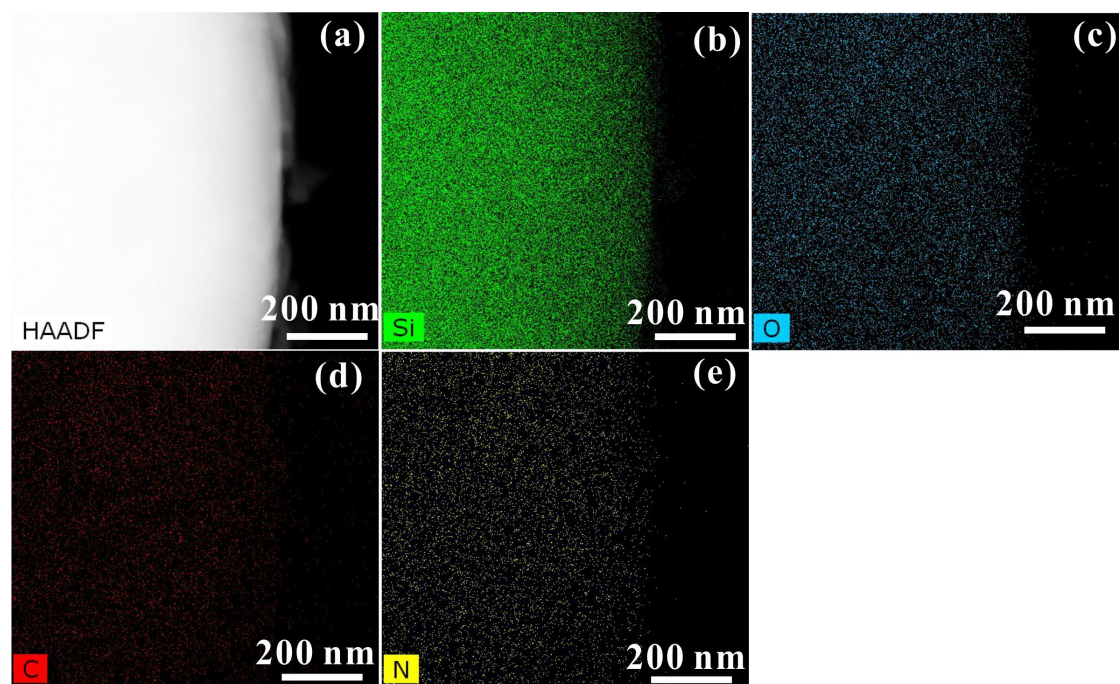| Samples	Si (at%)	O (at%)	C (at%)	N (at%)
SiOCN	19.16	23.29	49.13	8.42
SiO$_x$/NC	22.72	32.40	38.90	5.98
VG@ SiO$_x$/NC	1.16	11.63	86.99	0.22

Fig. S8 High angle annular dark field (HAADF) image (a) and corresponding EDS elemental mapping images of Si (b), O (c), C (d), and N (e) of crushed SiO$_x$/NC spheres.
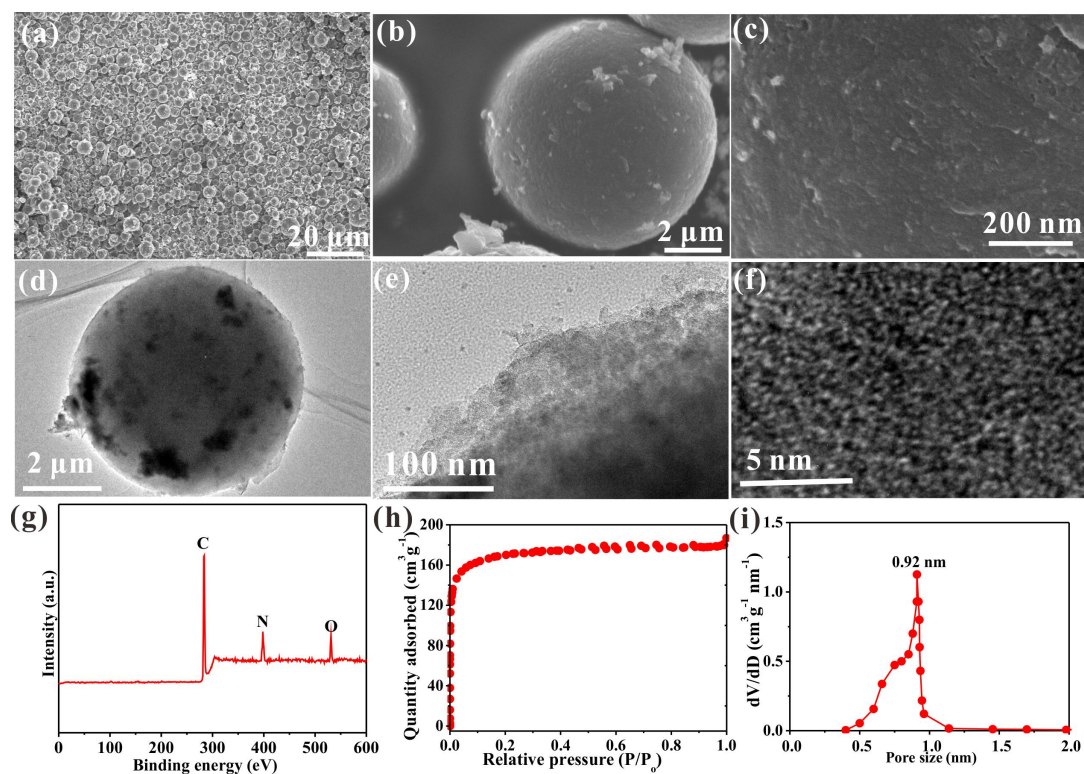
Fig. S9 (a-c) SEM images, (d-f) TEM images, (g) XPS survey spectrum, (h) Nitrogen adsorption-desorption isotherms, and (i) pore-size distribution calculated by BJH method of NC.
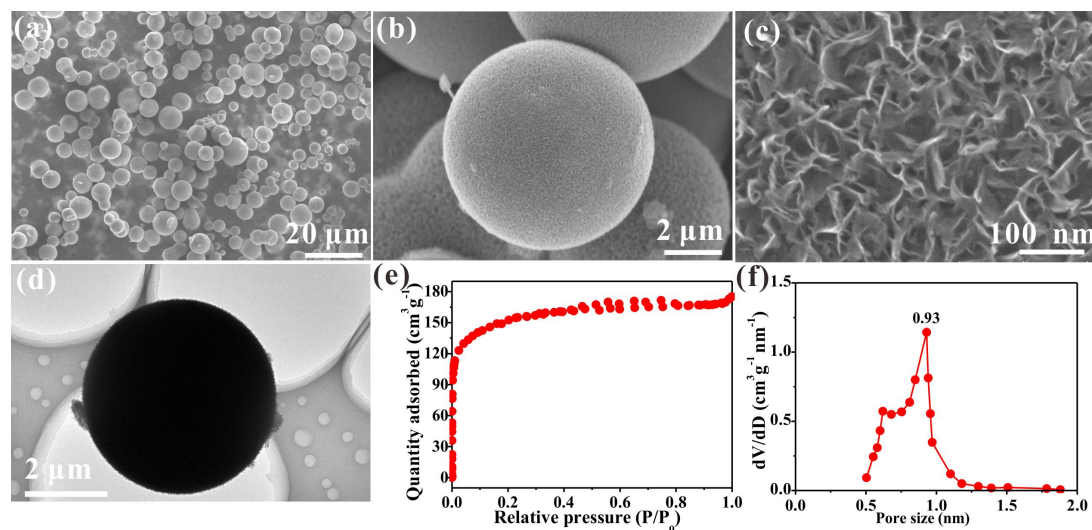

Fig. S10 (a-c) SEM images, (d) TEM image, (e) Nitrogen adsorption-desorption isotherms, and (f) pore-size distribution calculated by BJH method of VG@NC.
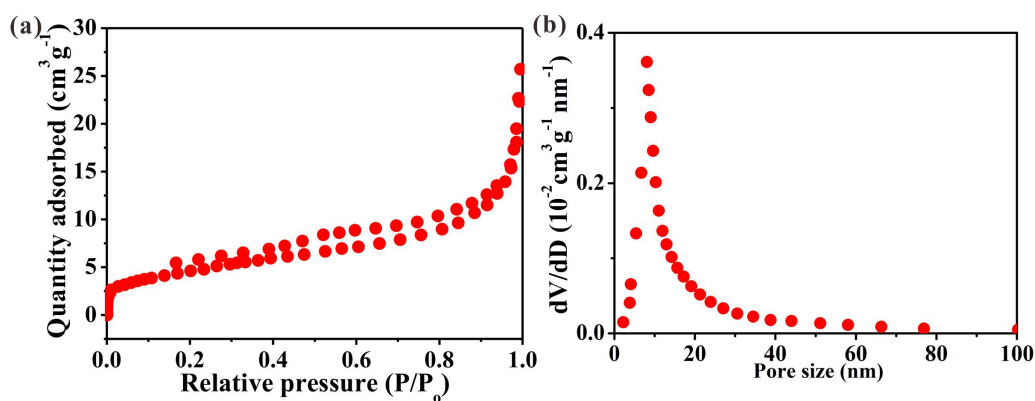
Fig. S11 (a) Nitrogen adsorption-desorption isotherms and (b) pore-size distribution calculated by BJH method of SiO_x/NC.

Fig. S12 (a) Charge/discharge curves of NC, (b) Charge/discharge curves of VG@NC, (c) Cycling curves of NC and VG@NC at a current density of 0.1 A g^{-1}, and (d) Rate performances of NC and VG@NC.

Fig. S13 (a,b) CV curves at different scanning rates of SiO_x/NC (a) and $VG@SiO_x/NC$ (b) after experiencing 100 cycles at a current density of 0.1 A g^{-1}, and (c,d) the peak current against the square root of scan rates for the SiO_x/NC (c) and $VG@SiO_x/NC$ (d).

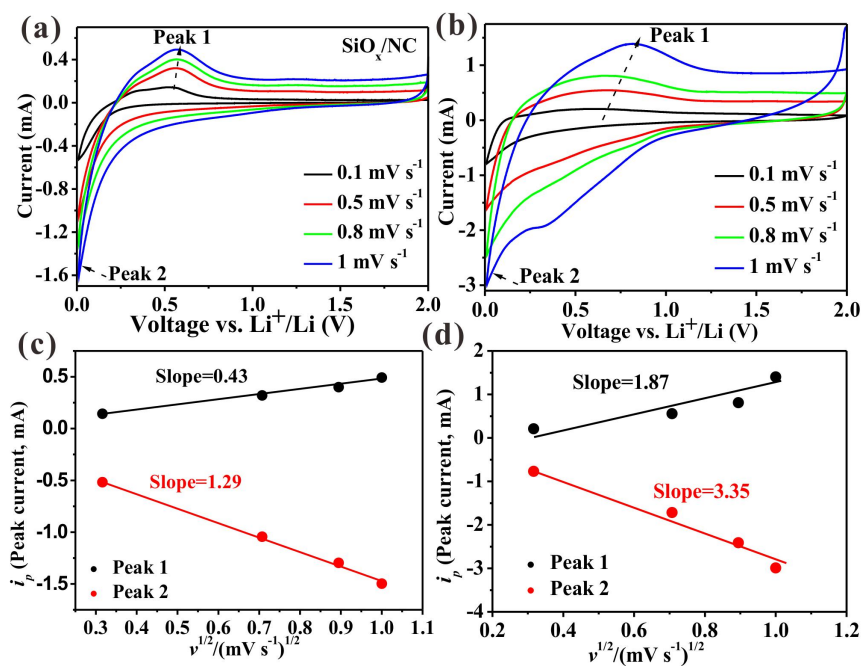**Table S3** Lithium ion storage performances of SiO_x ($0<x<2$) and its composites reported. The charge capacity mean those obtained in the final cycle. C_C-charge capacity (mAh g^{-1}), C_R-capacity retention (%), M_L-Mass loading (mg cm^{-2}), J-current density (A g^{-1}), N_C-cycle number, NA-not available.

Samples	C_C	C_R	M_L	J	N_C	References
VG@SiO$_x$/NC	1229.2	92.9	1.5	0.1	100	**This work**
VG@SiO$_x$/NC	641.9	84.2	1.5	2	500	**This work**
VG@SiO$_x$/NC	265.5	NA	1.5	20	NA	**This work**
Si@SiO$_x$/C	1361.9	83.3	3	0.2	100	*ACS Nano*, 2019, **13**, 9607−9619.
Si@SiO$_x$/C	1342	NA	3	4	NA	*ACS Nano*, 2019, **13**, 9607−9619.
Si/SiO$_x$–SiO	~780	80.7	1.2	0.2	350	*J. Mater. Chem. A*, 2019, **7**, 15621-15626.
Ni/SiO$_x$/N-doped C	~820	93.7	0.53	0.2	70	*J. Mater. Chem. A*, 2019, **7**, 15969-15974.
Ni/SiO$_x$/N-doped carbon	289.8	NA	0.53	10	NA	*J. Mater. Chem. A*, 2019, **7**, 15969-15974.
SiO$_x$/G/C	487	74.6	3.5	0.12	500	*Nano Energy*, 2019, **60**, 485-492.
SiO$_x$/G/C	582.5	NA	3.5	3	NA	*Nano Energy*, 2019, **60**, 485-492.
SiO$_x$/C	895	80.8	1.2	0.2	200	*J. Mater. Chem. A*, 2018, **6**, 14903-14909.
SiO$_x$/C	532	NA	1.2	2	NA	*J. Mater. Chem. A*, 2018, **6**, 14903-14909.
SiO$_x$/G	950	91.2	1.5	0.5	100	*Adv. Mater.* 2018, **30**, 1707430.
SiO$_x$/G	661	NA	1.5	10	NA	*Adv. Mater.* 2018, **30**, 1707430.
SiO$_x$/C	580	90	3.5	0.325	500	*Adv. Funct. Mater.* 2018, **28**, 1705235.
D-SiO/graphene	930	93	1.5	0.32	100	*Nano Lett.* 2017, **17**, 3681-3687.
Si-SiO$_x$-C	1034.6	77.6	1	1.03	200	*Nano Lett.* 2017, **17**, 1870-1876.
Si/C/SiOC	~193	NA	2.0	0.4	100	*ACS Nano* 2017, **11**, 11409-11416.